

Electronic Supplementary Information

Photoinduced Electron Transfer in Tris(2,2'-bipyridine)ruthenium(II)-Viologen Dyads with Peptide Backbones Leading to Long-Lived Charge Separation and Hydrogen Evolution

Makoto Ogawa,^a Bijitha Balan,^a Gopalakrishnan Ajayakumar,^a Shigeyuki Masaoka,^{a,b} Heinz-Bernhard Kraatz,^c Masayasu Muramatsu,^d Syoji Ito,^d Yutaka Nagasawa,^d Hiroshi Miyasaka,^d and Ken Sakai^{*a}

^a*Department of Chemistry, Faculty of Science, Kyushu University, Hakozaki 6-10-1, Higashiku, Fukuoka 812-8581, Japan.* ^b*PRESTO, Japan Science and Technology Agency (JST), Honcho 4-1-8, Kawaguchi, Saitama, 332-0012, Japan.* ^c*Department of Chemistry, The University of Western Ontario, 1151 Richmond Street, London, Ontario, Canada N6A 5B7.*

^d*Division of Frontier Materials Science, Graduate School of Engineering Science, Osaka University, Toyonaka, Osaka 560-8531, Japan.*

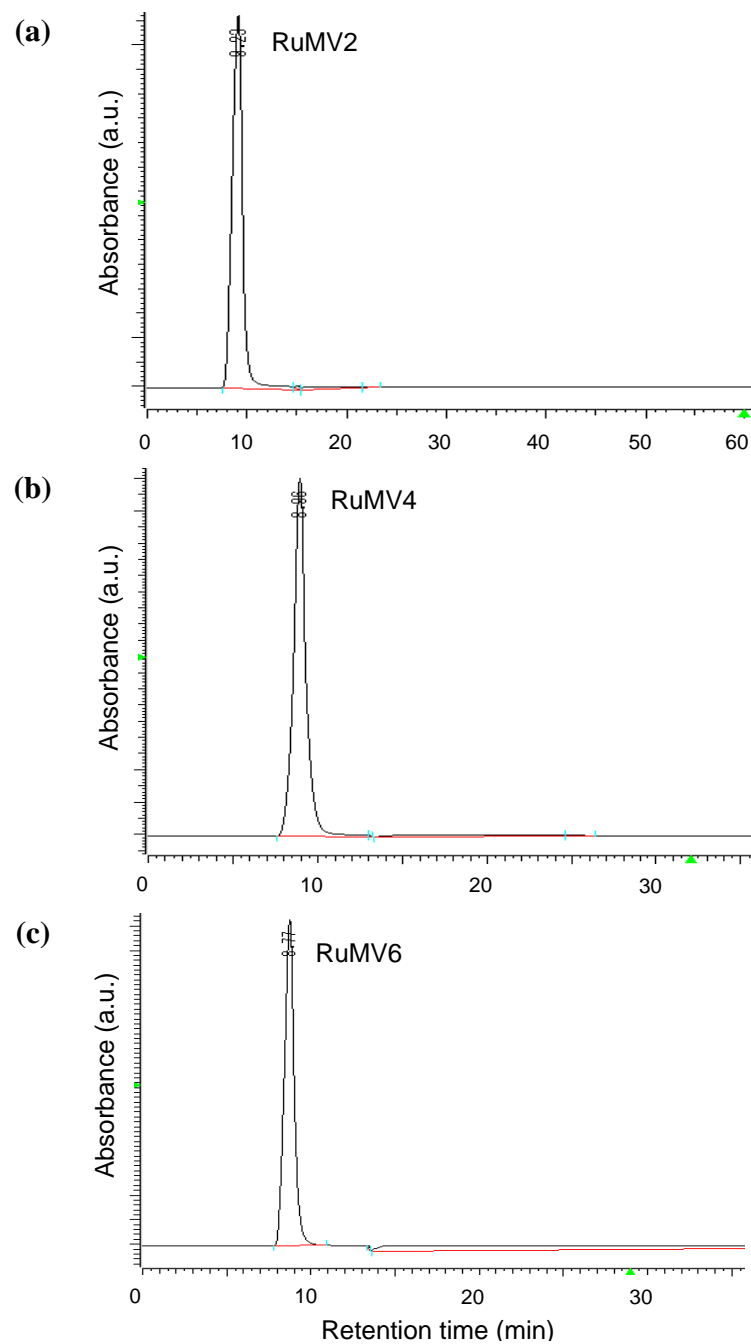


Fig. S1 HPLC traces of (a) **RuMV2**(PF₆)₆·2H₂O, (b) **RuMV4**(PF₆)₁₀·H₂O, and (c) **RuMV6**(PF₆)₁₄·H₂O. The HPLC purification together with the purity confirmation shown in these figures was performed on a C18 column using a water/acetonitrile mixture as the eluent. The linear gradient changed from 5 to 95% in the acetonitrile content over 40 min at a flow rate of 0.1 mL/min.

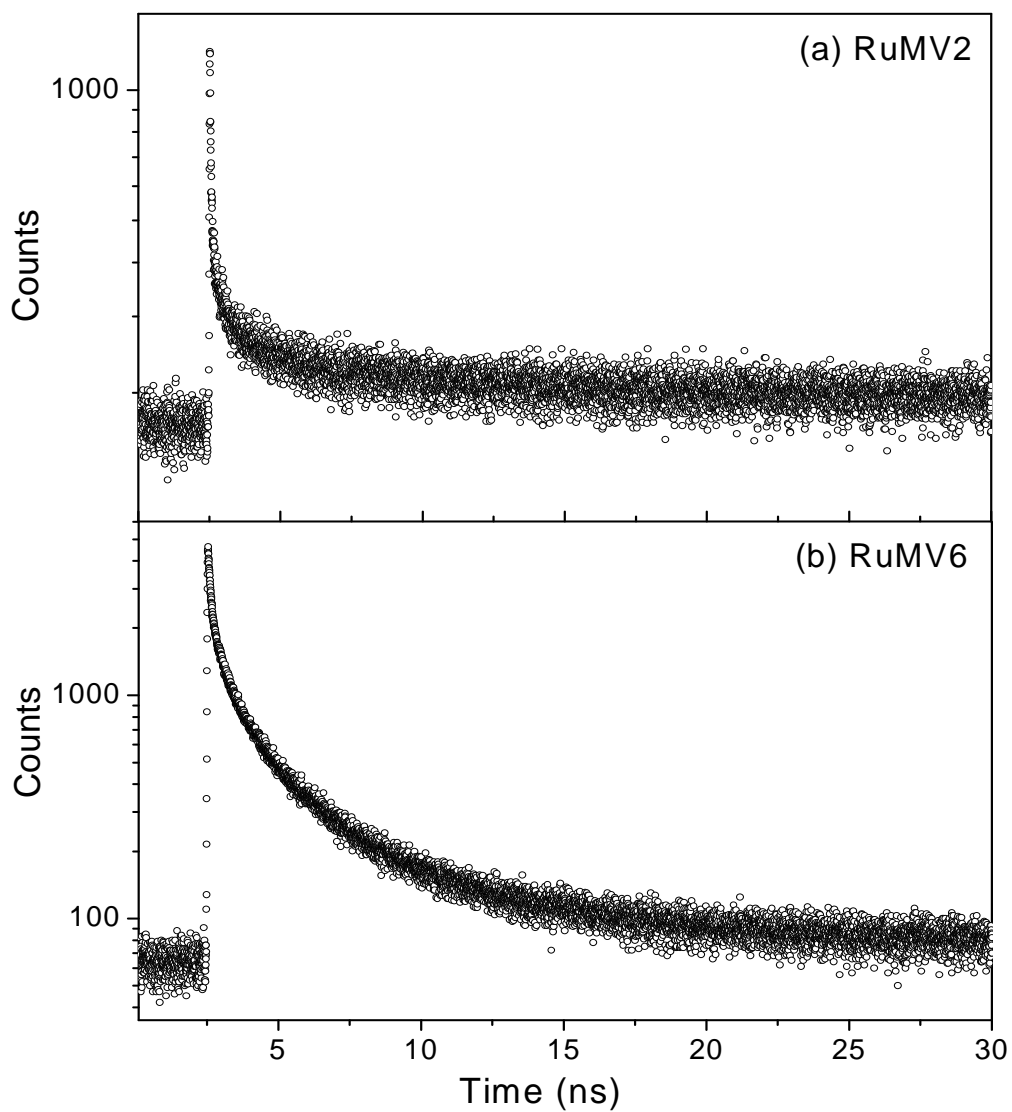


Fig. S2 Emission decay profiles of (a) **RuMV2**(PF₆)₆·2H₂O and (b) **RuMV6**(PF₆)₁₄·H₂O in water under a deaerated condition, at room temperature obtained by the time correlated single photon counting (TC-SPC) methods. The excitation source was a double-frequency Nd:YAG laser (532 nm). The emission was monitored at 610 nm.

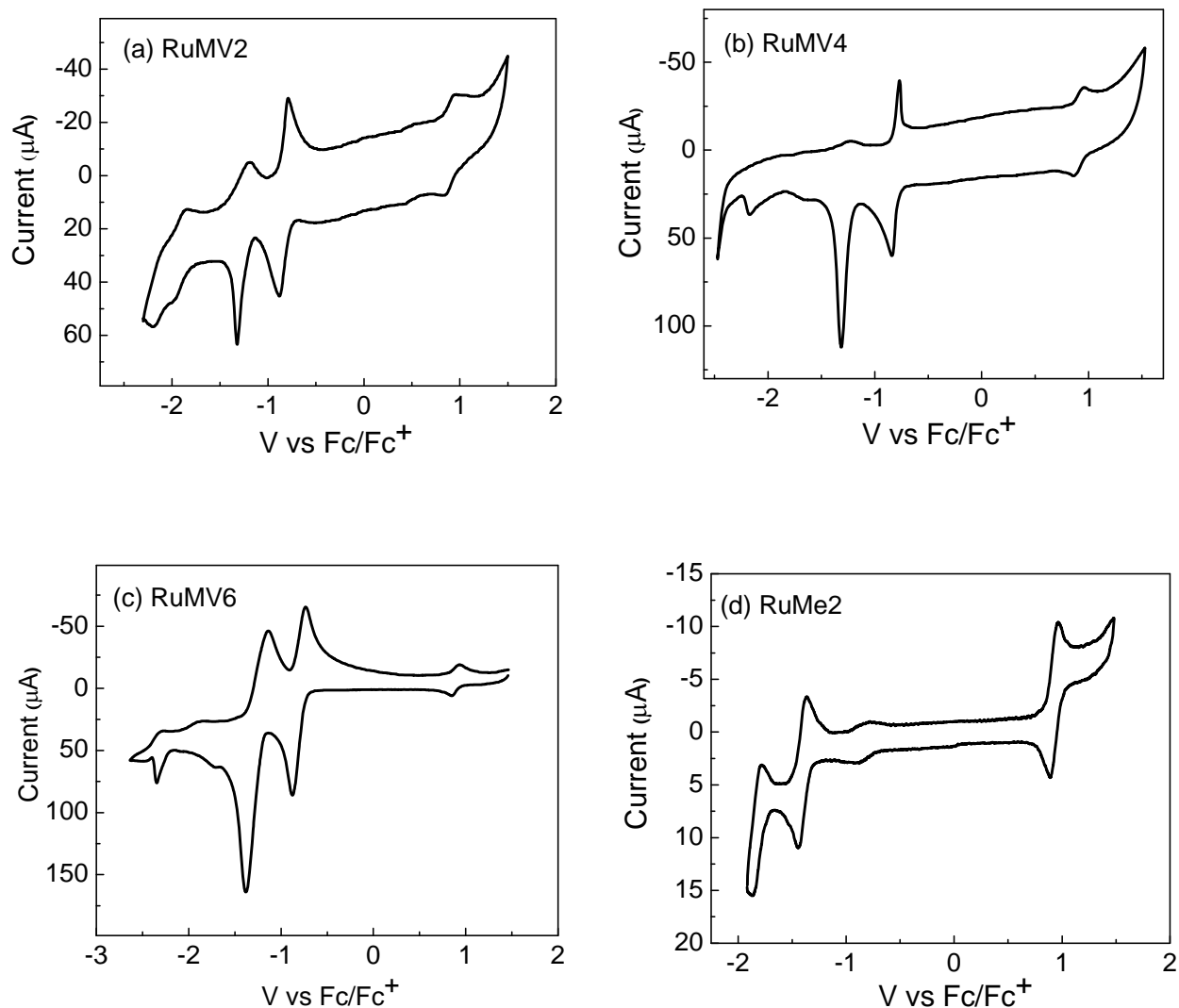


Fig. S3 Cyclic voltammograms of (a) **RuMV2**(PF₆)₆·2H₂O, (b) **RuMV4**(PF₆)₁₀·H₂O, (c) **RuMV6**(PF₆)₁₄·H₂O, and (d) **RuMe2**(PF₆)₂·H₂O (1 mM) in an acetonitrile solution containing 0.1 M TBAP (TBAP = tetra(n-butyl)ammonium perchlorate) at room temperature under Ar atmosphere. Each voltammogram was recorded at a sweep rate of 50 mVs⁻¹.

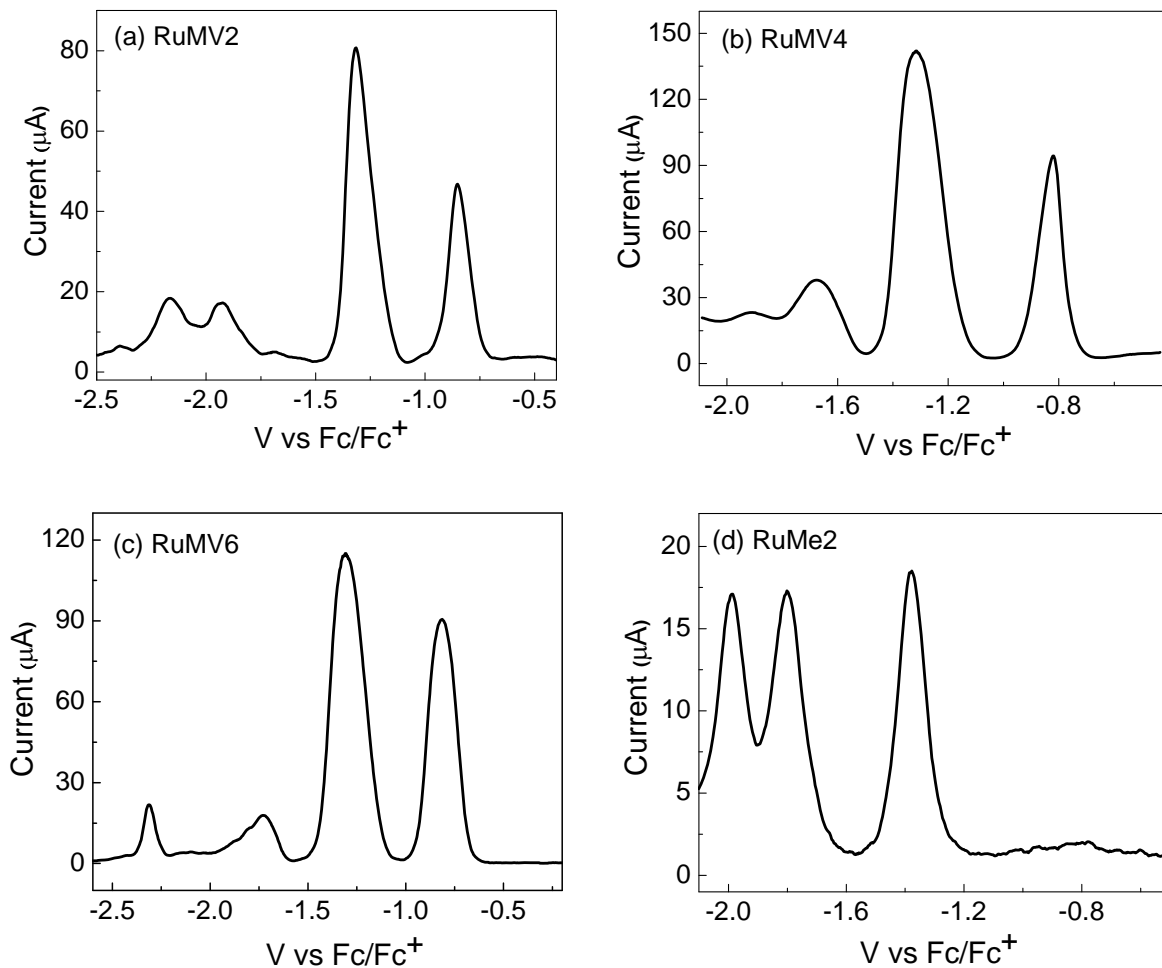


Fig. S4 Differential pulse voltammograms of (a) **RuMV2** $(\text{PF}_6)_6 \cdot 2\text{H}_2\text{O}$, (b) **RuMV4** $(\text{PF}_6)_{10} \cdot \text{H}_2\text{O}$, (c) **RuMV6** $(\text{PF}_6)_{14} \cdot \text{H}_2\text{O}$, and (d) **RuMe2** $(\text{PF}_6)_2 \cdot \text{H}_2\text{O}$ (1 mM) in an acetonitrile solution containing 0.1 M TBAP (TBAP = tetra(n-butyl)ammonium perchlorate) at room temperature under Ar atmosphere. Each voltammogram was recorded using a glassy carbon disk as the working electrode, at a sweep rate of 50 mVs^{-1} , a potential amplitude of 50 mV, and a step height of 4 mV.

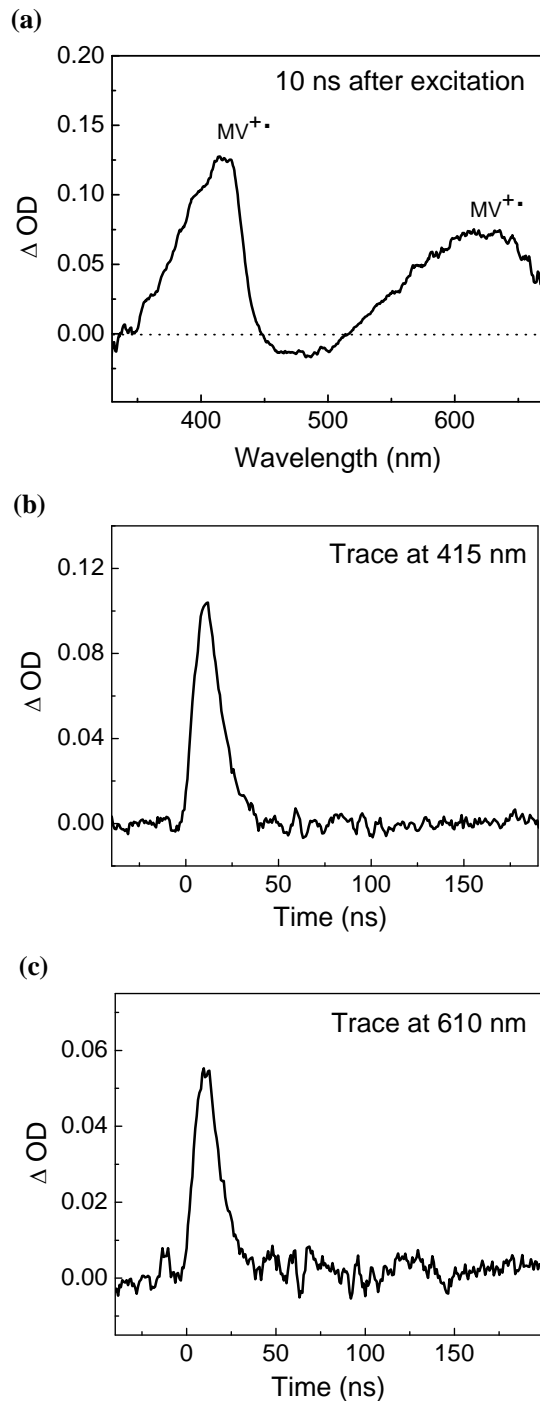


Fig. S5 (a) Nanosecond transient absorption spectrum of **RuMV2(PF₆)₆·2H₂O** in water followed by excitation using a 532-nm laser source (10 ns after the laser pulse). Transient traces at (b) 415 nm and (c) 610 nm corresponding to the behavior of MV^{•+} are also shown.

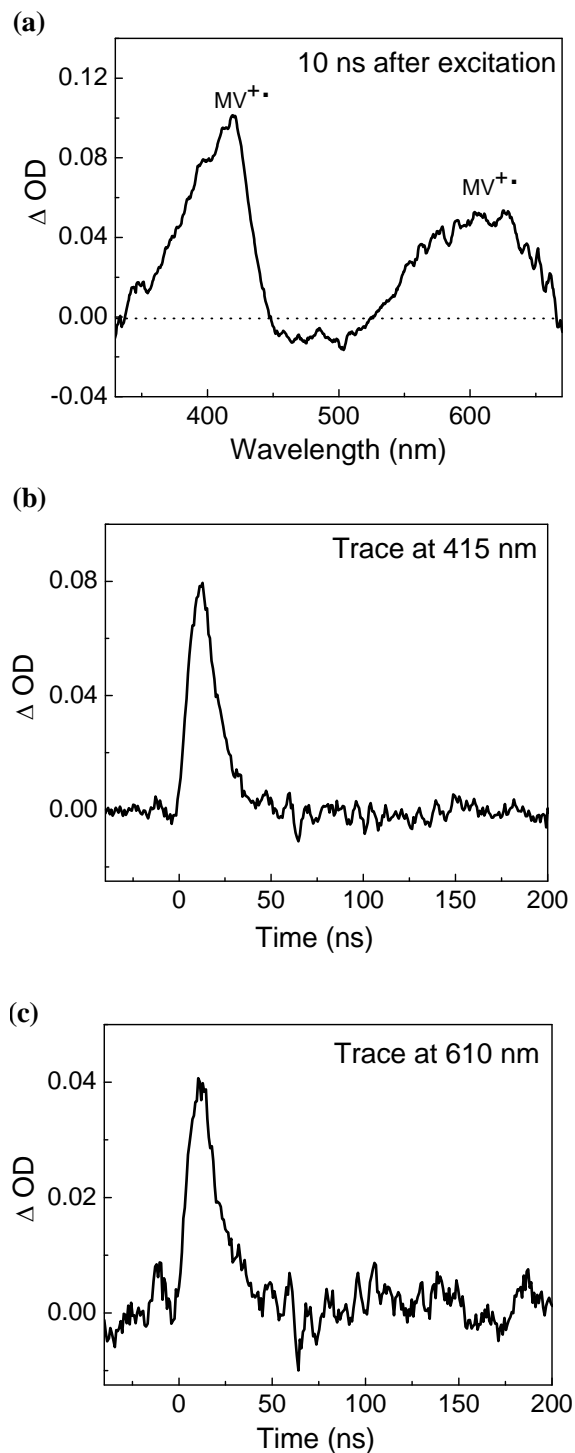


Fig. S6 (a) Nanosecond transient absorption spectrum of **RuMV6(PF₆)₁₄·H₂O** in water followed by excitation using a 532-nm laser source (10 ns after the laser pulse). Transient traces at (b) 415 nm and (c) 610 nm corresponding to the behavior of $MV^{+}\cdot$ are also shown.

Conductivity Measurements

The molar conductivities of aqueous solutions of the **RuMVn** complexes were measured as a function of the total complex concentration. Measurements were carried out using a TOA CM-20S conductometer with a CG-511B type conductivity cell having a cell constant of 0.969 cm⁻¹. The cell constant was determined using a standard solution containing 1.0 mM KCl. The values higher than *ca.* 5 mS/m were adopted, while those below this threshold were abandoned. The conductivity data were measured for all the PF₆⁻ salts of the **RuMV2-RuMV6** complexes, together with the chloride salt of the **RuMV4** complex, and are summarized in Tables S1-S4. To ascertain the validity of our experimental techniques and also to obtain rough estimates for the molar conductivities of Ru(bpy)₃²⁺ and MV²⁺ under the present experimental conditions, the measurements were also carried out for KCl, [Ru(bpy)₃]Cl₂·6H₂O, and [MV]Cl₂·3H₂O. The molar conductivity of [Ru(bpy)₃]Cl₂ varied in the range $\frac{1}{2}\{\Lambda([Ru(bpy)_3]Cl_2)\} = 121\sim 134$ Scm²mol⁻¹ when the concentration was changed from 1.0 to 0.25 mM, while that of [MV]Cl₂ varied in the range $\frac{1}{2}\{\Lambda(MVCl_2)\} = 160\sim 161$ Scm²mol⁻¹ upon changing the concentration from 1.0 to 0.25 mM. Since the molar conductivity of a salt is given by the sum of the molar conductivities of the cationic and anionic species (e.g., $\Lambda(KCl) = \lambda(K^+) + \lambda(Cl^-)$), the equivalent molar conductivities of [Ru(bpy)₃]²⁺ and MV²⁺ are estimated as $\frac{1}{2}\{\lambda(Ru(bpy)_3^{2+})\} = 45\sim 58$ Scm²mol⁻¹ and $\frac{1}{2}\{\lambda(MV^{2+})\} = 85$ Scm²mol⁻¹, respectively, where the molar conductivity of Cl⁻ was taken from the literature ($\lambda(Cl^-) = 76.4$ Scm²mol⁻¹)¹ and was used in these estimations. The former values for Ru(bpy)₃²⁺ are roughly consistent with its literature value $\frac{1}{2}\{\lambda(Ru(bpy)_3^{2+})\} = 36.9$ Scm²mol⁻¹.² It is rather important to note here that the value estimated for $\frac{1}{2}\{\lambda(MV^{2+})\}$ is quite consistent with the value of $\frac{1}{(z-m)}\{\lambda(RuMVn(PF_6)_{m^{(z-m)}}^+)\}$, which was estimated as 88 Scm²mol⁻¹ in the following simulation studies.

From the mass balance with regard to the **RuMVn** complex, the total concentration of the **RuMVn(X)_m^{(z-m)+}** species ($m = 0, 1, 2, \dots, z$) is given by equation (S-1),

$$[A]_t = [A^{z+}] + [AX^{(z-1)+}] + [AX_2^{(z-2)+}] + \dots + [AX_{z-1}^+] + [AX_z] \quad (S-1)$$

where A denotes each **RuMVn** cation, and [A]_t denotes the total concentration of AX_m dissolved in each experiment (abbreviated as C_t). By use of the total stability constants ($\beta_1, \beta_2, \dots, \beta_z$), equation (S-1) can be transformed into the following equation,

$$C_t = [A^{z+}](1 + \beta_1x + \beta_2x^2 + \dots + \beta_zx^z) \quad (S-2)$$

where x denotes the concentration of the counter anion, i.e. $[X^-]$, in solution ($X^- = \text{PF}_6^-$, Cl^- , etc.). On the other hand, the following equation can also be derived based on the mass balance with regard to the counter anion involved in the system.

$$z[A]_t = [X^-] + [AX^{(z-1)+}] + 2[AX_2^{(z-2)+}] + \dots + (z-1)[AX_{z-1}^+] + z[AX_z] \quad (\text{S-3})$$

This can be similarly transformed into the following equation.

$$zC_t = x + \beta_1 x[A^{z+}] + 2\beta_2 x^2[A^{z+}] + 3\beta_3 x^3[A^{z+}] + \dots + (z-1)\beta_{z-1} x^{z-1}[A^{z+}] + z\beta_z x^z[A^{z+}] \quad (\text{S-4})$$

From equations (S-2) and (S-4), the following equation (S-5) is given.

$$\frac{C_t}{zC_t - x} = \frac{1 + \beta_1 x + \beta_2 x^2 + \dots + \beta_z x^z}{\beta_1 x + 2\beta_2 x^2 + 3\beta_3 x^3 + \dots + (z-1)\beta_{z-1} x^{z-1} + z\beta_z x^z} \quad (\text{S-5})$$

The apparent molar conductivity is given by the following equation,

$$\Lambda = \frac{1}{C_t} \{(\lambda(X^-)x + \lambda(A^{z+})[A^{z+}] + \lambda(AX^{(z-1)+})[AX^{(z-1)+}] + \dots + \lambda(AX_{z-1}^+)[AX_{z-1}^+])\} \quad (\text{S-6})$$

where Λ is the apparent molar conductivity of each salt, $\lambda(X^-)$ denotes the molar conductivity of the counter anion ($X^- = \text{PF}_6^-$ or Cl^-), and $\lambda(AX_m^{(z-m)+})$ corresponds to that of an $AX_m^{(z-m)+}$ cation ($m = 0, 1, 2, \dots, z-1$).

For simplicity, we further decided to suppose that all the cationic species involving each **RuMVn** cation have the same mobility in aqueous media. Thus, it is supposed that the following equations are satisfied.

$$\begin{aligned}
 \lambda(A^{z+}) &\doteq z \lambda(AX_{z-1}^+) \\
 \lambda(AX^{(z-1)+}) &\doteq (z-1)\lambda(AX_{z-1}^+) \\
 \lambda(AX_2^{(z-2)+}) &\doteq (z-2)\lambda(AX_{z-1}^+) \\
 &\vdots \\
 &\vdots \\
 &\vdots \\
 \lambda(AX_{z-2}^{2+}) &\doteq 2 \lambda(AX_{z-1}^+)
 \end{aligned}
 \quad \left. \right\} \text{(S-7)}$$

By applying (S-7) to (S-6), the apparent molar conductivity can be expressed by the following equations.

$$\begin{aligned}
 \Lambda &= \frac{1}{C_t} \{ (\lambda(X^-) x + z\lambda(AX_{z-1}^+)[A^{z+}] + (z-1)\lambda(AX_{z-1}^+)[AX^{(z-1)+}] + \dots \\
 &\quad \dots \dots + 2\lambda(AX_{z-1}^+)[AX_{z-2}^{2+}] + \lambda(AX_{z-1}^+)[AX_{z-1}^{+}]) \} \\
 &= \frac{1}{C_t} \{ \lambda(X^-) x + \lambda(AX_{z-1}^+) (z[A^{z+}] + (z-1)[AX^{(z-1)+}] + \dots \\
 &\quad \dots \dots + 2[AX_{z-2}^{2+}] + [AX_{z-1}^{+}]) \} \\
 &= \frac{1}{C_t} \{ \lambda(X^-) x + \lambda(AX_{z-1}^+)[A^{z+}](z + (z-1)\beta_1 x + \dots \\
 &\quad \dots \dots + 2\beta_{z-2}x^{z-2} + \beta_{z-1}x^{z-1}) \}
 \end{aligned} \quad \text{(S-8)}$$

Furthermore, $[A^{z+}]$ is given by the following equation.

$$[A^{z+}] = \frac{C_t}{1 + \beta_1 x + \beta_2 x^2 + \dots + \beta_z x^z} \quad \text{(S-9)}$$

By supposing an appropriate set of total stability constants, the concentration of X^- (i.e., x) can be calculated at each total concentration of the **RuMVn** complex, C_t . By use of our original simulation program developed for this purpose, we could successfully regenerate the observed

molar conductivity data. In the simulation, we adopted the following scheme to define an appropriate set of stepwise formation constants ($K_1, K_2, K_3, \dots, K_z$) for each system.

$$\frac{K_2}{K_1} = \frac{K_3}{K_2} = \frac{K_4}{K_3} = \frac{K_5}{K_4} = \dots = \frac{K_z}{K_{z-1}} = \alpha \quad (\text{S-10})$$

This is a reasonable scheme considering the fact that the major contribution to the free energy change in each step correlates with the coulombic attraction and is therefore considered proportional to the number of positive charge (z) of the cation which forms an ion pair with X^- . The stepwise formation constants together with the total stability constants used to simulate the observed data are summarized in Table S5.

The molar conductivities of PF_6^- and Cl^- ($59.2 \text{ Scm}^2\text{mol}^{-1}$ and $76.4 \text{ Scm}^2\text{mol}^{-1}$, respectively) were taken from the literatures^{1,3} and were adopted in all the simulation studies. The equivalent molar conductivities (λ_0/z_i , λ_0 is the molar conductivity of each cationic species and the z_i denotes the number of positive charge of the cation) of all the $\text{AX}_m^{(z-m)+}$ cations were fixed at $\lambda(\text{AX}_m^{(z-m)+})/(z-m) = 88 \text{ Scm}^2\text{mol}^{-1}$, since this value well reproduced all the observed data and also found consistent with $\frac{1}{2}\{\lambda(\text{MV}^{2+})\} = 85 \text{ Scm}^2\text{mol}^{-1}$. The calculated lines given from these simulation experiments are all given in Fig. 7. The numerical data obtained in these simulation experiments are all listed in Table S6. By adopting the stability constants summarized in Table S5, the relative abundances of all the $\text{AX}_m^{(z-m)+}$ species in aqueous media can be calculated as shown in Figs. S7-S10. Finally, the relative abundances of all the chemical species in solution under the reported spectroscopic and photolysis conditions are given in Tables S7-S10.

The simulation program (including the source codes), developed by using the Delphi 5 package under the Windows platform, is also supplied as supporting information (a single zip file: conductivity_simulation.zip). It can be also downloaded at the author's website: <http://www.scc.kyushu-u.ac.jp/Sakutai/softwares/softwares.eng.html>

Table S1 The observed molar conductivity of **RuMV2(PF₆)₆·2H₂O** in water vs. the square root of the total concentration.

$C^{1/2}$ (mM ^{1/2})	Λ (Scm ² mol ⁻¹)
0.02388	543.9
0.01639	566.1
0.01245	633.6
0.01000	687.0

Table S2 The observed molar conductivity of **RuMV4(PF₆)₁₀·H₂O** in water vs. the square root of the total concentration.

$C^{1/2}$ (mM ^{1/2})	Λ (Scm ² mol ⁻¹)
0.02236	688.0
0.01583	730.5
0.01217	824.3
0.009950	899.0
0.006964	1052

Table S3 The observed molar conductivity of **RuMV4(Cl)₁₀** in water vs. the square root of the total concentration.

$C^{1/2}$ (mM ^{1/2})	Λ (Scm ² mol ⁻¹)
0.02276	1004
0.01972	997.4
0.01577	1074
0.01123	1198
0.008683	1283
0.007036	1400

Table S4 The observed molar conductivity of **RuMV6(PF₆)₁₄·H₂O** in water vs. the square root of the total concentration.

$C^{1/2}$ (mM ^{1/2})	Λ (Scm ² mol ⁻¹)
0.02034	1027
0.01417	1121
0.01093	1244
0.008906	1398
0.006244	1570

Table S5 The α values for eq. (S-10), the stepwise formation constants, and the total stability constants used to simulate the conductivity data.

Params	RuMV2(PF₆)₆·2H₂O	RuMV4(PF₆)₁₀·H₂O	RuMV6(PF₆)₁₄·H₂O	RuMV4(Cl)₁₀
α	0.20	0.50	0.56	0.43
K_1 (β_1)	1.0×10^4 (1.0×10^4)	1.5×10^4 (1.5×10^4)	1.5×10^4 (1.5×10^4)	6.4×10^3 (6.4×10^3)
K_2 (β_2)	2000 (2.000×10^7)	7500 (1.125×10^8)	8400 (1.26×10^8)	2752 (1.76×10^8)
K_3 (β_3)	400.0 (8.000×10^9)	3750 (4.219×10^{11})	4704 (5.93×10^{11})	1183 (2.08×10^{10})
K_4 (β_4)	80.00 (6.400×10^{11})	1875 (7.910×10^{14})	2634 (1.56×10^{15})	508.8 (1.06×10^{13})
K_5 (β_5)	16.00 (1.024×10^{13})	937.5 (7.416×10^{17})	1475 (2.30×10^{18})	218.8 (2.32×10^{15})
K_6 (β_6)	3.200 (3.277×10^{13})	468.8 (3.476×10^{20})	826.1 ($.90 \times 10^{21}$)	94.09 (2.18×10^{17})
K_7 (β_7)		234.4 (8.147×10^{22})	462.6 (8.80×10^{23})	40.46 (8.83×10^{18})
K_8 (β_8)		117.2 (9.548×10^{24})	259.1 (2.28×10^{26})	17.40 (1.54×10^{20})
K_9 (β_9)		58.59 (5.594×10^{26})	145.1 (3.31×10^{28})	7.480 (1.15×10^{21})
K_{10} (β_{10})		29.30 (1.639×10^{28})	81.25 (2.69×10^{30})	3.217 (3.70×10^{21})
K_{11} (β_{11})			45.50 (1.22×10^{32})	
K_{12} (β_{12})			25.48 (3.12×10^{33})	
K_{13} (β_{13})			14.27 (4.44×10^{34})	
K_{14} (β_{14})			7.990 (3.55×10^{35})	

Table S6 The numerical data obtained by the simulation experiments.

RuMV2(PF₆)₆·2H₂O		RuMV4(PF₆)₁₀·H₂O		RuMV6(PF₆)₁₄·H₂O		RuMV4(Cl)₁₀	
<i>C</i> ^{1/2} (mM ^{1/2})	<i>A</i> (S cm ² mol ⁻¹)	<i>C</i> ^{1/2} (mM ^{1/2})	<i>A</i> (S cm ² mol ⁻¹)	<i>C</i> ^{1/2} (mM ^{1/2})	<i>A</i> (S cm ² mol ⁻¹)	<i>C</i> ^{1/2} (mM ^{1/2})	<i>A</i> (S cm ² mol ⁻¹)
0.002130	848.6	0.001995	1390	0.001815	1959	0.002031	1599
0.003012	824.1	0.002821	1325	0.002567	1875	0.002872	1564
0.003689	804.7	0.003456	1274	0.003144	1809	0.003517	1533
0.004260	788.9	0.003990	1232	0.003630	1755	0.004061	1505
0.004763	775.4	0.004461	1197	0.004058	1710	0.004541	1481
0.005218	763.7	0.004887	1168	0.004446	1672	0.004974	1458
0.005636	753.4	0.005278	1142	0.004802	1640	0.005373	1439
0.006025	744.2	0.005643	1119	0.005133	1611	0.005743	1420
0.006390	735.9	0.005985	1099	0.005445	1586	0.006092	1404
0.006736	728.3	0.006309	1081	0.005739	1563	0.006421	1388
0.007065	721.4	0.006617	1064	0.006019	1543	0.006735	1374
0.007379	715.0	0.006911	1049	0.006287	1524	0.007034	1361
0.007680	709.0	0.007193	1035	0.006544	1506	0.007322	1349
0.007970	703.4	0.007465	1023	0.006791	1490	0.007598	1337
0.008250	698.2	0.007727	1011	0.007029	1476	0.007865	1326
0.008520	693.3	0.007980	999.3	0.007260	1462	0.008122	1316
0.008783	688.7	0.008226	988.8	0.007483	1449	0.008372	1306
0.009037	684.3	0.008464	978.8	0.007700	1436	0.008615	1297

(Contd.)

Table S6 (Contd.)

0.009285	680.1	0.008696	969.5	0.007911	1425	0.008851	1288
0.009526	676.2	0.008922	960.6	0.008117	1414	0.009081	1280
0.009761	672.4	0.009142	952.1	0.008317	1403	0.009305	1272
0.009991	668.8	0.009358	944.1	0.008513	1393	0.009524	1265
0.01022	665.3	0.009568	936.4	0.008704	1384	0.009739	1257
0.01044	662.0	0.009774	929.1	0.008891	1375	0.009948	1250
0.01065	658.8	0.009975	922.1	0.009075	1366	0.01015	1244
0.01086	655.7	0.01017	915.3	0.009254	1357	0.01035	1237
0.01107	652.8	0.01037	908.8	0.009431	1349	0.01055	1231
0.01127	649.9	0.01056	902.6	0.009604	1342	0.01075	1225
0.01147	647.2	0.01074	896.6	0.009774	1334	0.01094	1219
0.01167	644.5	0.01093	890.8	0.009941	1327	0.01112	1214
0.01186	641.9	0.01111	885.2	0.01011	1320	0.01131	1208
0.01205	639.4	0.01129	879.7	0.01027	1313	0.01149	1203
0.01224	637.0	0.01146	874.5	0.01043	1307	0.01167	1198
0.01242	634.7	0.01163	869.4	0.01058	1300	0.01184	1193
0.01260	632.4	0.01180	864.5	0.01074	1294	0.01201	1188
0.01278	630.2	0.01197	859.7	0.01089	1288	0.01218	1183
0.01296	628.0	0.01214	855.0	0.01104	1282	0.01235	1179
0.01313	625.9	0.01230	850.5	0.01119	1277	0.01252	1174
0.01330	623.9	0.01246	846.1	0.01133	1271	0.01268	1170
0.01347	621.9	0.01262	841.2	0.01148	1266	0.01284	1166

(Contd.)

Table S6 (Contd.)

0.01364	619.9	0.01277	837.6	0.01162	1261	0.01300	1162
0.01381	618.0	0.01293	833.5	0.01176	1256	0.01316	1158
0.01397	616.2	0.01308	829.6	0.01190	1251	0.01332	1154
0.01413	614.4	0.01323	825.7	0.01204	1246	0.01347	1150
0.01429	612.6	0.01338	821.9	0.01218	1241	0.01362	1147
0.01445	610.9	0.01353	818.2	0.01231	1236	0.01377	1143
0.01460	609.2	0.01368	814.6	0.01244	1232	0.01392	1139
0.01476	607.5	0.01382	811.0	0.01257	1228	0.01407	1136
0.01491	605.9	0.01397	807.6	0.01270	1223	0.01421	1132
0.01506	604.3	0.01411	804.2	0.01283	1219	0.01436	1129
0.01521	602.7	0.01425	800.8	0.01296	1215	0.01450	1126
0.01536	601.2	0.01439	797.6	0.01309	1211	0.01464	1123
0.01551	599.7	0.01452	794.4	0.01321	1207	0.01478	1119
0.01565	598.2	0.01466	791.3	0.01334	1203	0.01492	1116
0.01580	596.8	0.01480	788.2	0.01346	1199	0.01506	1113
0.01594	595.4	0.01493	785.2	0.01358	1195	0.01520	1110
0.01608	594.0	0.01506	782.2	0.01370	1192	0.01533	1107
0.01622	592.6	0.01519	779.3	0.01382	1188	0.01547	1105
0.01636	591.3	0.01532	776.5	0.01394	1184	0.01560	1102
0.01650	589.9	0.01545	773.7	0.01406	1181	0.01573	1099
0.01664	588.6	0.01558	770.9	0.01418	1177	0.01586	1096
0.01677	587.4	0.01571	768.2	0.01429	1174	0.01599	1094

(Contd.)

Table S6 (Contd.)

0.01691	586.1	0.01584	765.6	0.01441	1171	0.01612	1091
0.01704	584.9	0.01596	763.0	0.01452	1167	0.01625	1088
0.01717	583.6	0.01608	760.4	0.01463	1164	0.01637	1086
0.01731	582.4	0.01621	757.9	0.01474	1161	0.01650	1083
0.01744	581.3	0.01633	755.4	0.01486	1158	0.01662	1081
0.01757	580.1	0.01645	752.9	0.01497	1155	0.01675	1078
0.01769	578.9	0.01657	750.5	0.01508	1152	0.01687	1076
0.01782	577.8	0.01669	748.1	0.01519	1149	0.01699	1074
0.01795	576.7	0.01681	745.8	0.01529	1146	0.01711	1071
0.01807	575.6	0.01693	743.5	0.01540	1143	0.01723	1069
0.01820	574.5	0.01705	741.2	0.01551	1140	0.01735	1067
0.01832	573.4	0.01716	739.0	0.01561	1137	0.01747	1064
0.01845	572.4	0.01728	736.8	0.01572	1134	0.01759	1062
0.01857	571.4	0.01739	734.6	0.01582	1132	0.01770	1060
0.01869	570.3	0.01751	732.4	0.01593	1129	0.01782	1058
0.01881	569.3	0.01762	730.3	0.01603	1126	0.01793	1056
0.01893	568.3	0.01773	728.2	0.01613	1124	0.01805	1054
0.01905	567.3	0.01784	726.1	0.01623	1121	0.01816	1052
0.01917	566.4	0.01796	724.1	0.01633	1118	0.01828	1050
0.01929	565.4	0.01807	722.1	0.01644	1116	0.01839	1048
0.01941	564.4	0.01818	720.1	0.01654	1113	0.01850	1046
0.01952	563.5	0.01829	718.1	0.01663	1111	0.01861	1044

(Contd.)

Table S6 (Contd.)

0.01964	562.6	0.01839	716.2	0.01673	1109	0.01872	1042
0.01975	561.7	0.01850	714.3	0.01683	1106	0.01883	1040
0.01987	560.7	0.01861	712.4	0.01693	1104	0.01894	1038
0.01998	559.9	0.01872	710.5	0.01703	1101	0.01905	1036
0.02010	559.0	0.01882	708.7	0.01712	1099	0.01916	1034
0.02021	558.1	0.01893	706.9	0.01722	1097	0.01926	1032
0.02032	557.2	0.01903	705.1	0.01731	1094	0.01937	1031
0.02043	556.4	0.01914	703.3	0.01741	1092	0.01948	1029
0.02054	555.5	0.01924	701.5	0.01750	1090	0.01958	1027
0.02065	554.7	0.01934	699.8	0.01760	1088	0.01969	1025
0.02076	553.9	0.01945	698.1	0.01769	1086	0.01979	1024
0.02087	553.0	0.01955	696.4	0.01778	1083	0.01990	1022
0.02098	552.2	0.01965	694.7	0.01788	1081	0.02000	1020
0.02109	551.4	0.01975	693.0	0.01797	1079	0.02010	1019
0.02119	550.6	0.01985	691.4	0.01806	1077	0.02020	1017
0.02130	549.8	0.01995	689.7	0.01815	1075	0.02031	1015
0.02141	549.1	0.02005	688.1	0.01824	1073	0.02041	1014
0.02151	548.3	0.02015	686.5	0.01833	1071	0.02051	1012
0.02162	547.5	0.02025	684.9	0.01842	1069	0.02061	1010
0.02172	546.8	0.02035	683.4	0.01851	1067	0.02071	1009
0.02183	546.0	0.02044	681.8	0.01860	1065	0.02081	1007
0.02193	545.3	0.02054	680.3	0.01869	1063	0.02091	1006

(Contd.)

Table S6 (Contd.)

0.02203	544.6	0.02064	678.8	0.01877	1061	0.02101	1004
0.02214	543.8	0.02073	677.3	0.01886	1059	0.02110	1003
0.02224	543.1	0.02083	675.8	0.01895	1057	0.02120	1001
0.02234	542.4	0.02092	674.3	0.01904	1056	0.02130	999.7
0.02244	541.7	0.02102	672.9	0.01912	1054	0.02139	998.2
0.02254	541.0	0.02111	671.4	0.01921	1052	0.02149	996.7
0.02264	540.3	0.02121	670.0	0.01929	1050	0.02159	995.3
0.02274	539.6	0.02130	668.6	0.01938	1048	0.02168	993.9
0.02284	538.9	0.02139	667.2	0.01946	1046	0.02178	992.4
0.02294	538.2	0.02149	665.8	0.01955	1045	0.02187	991.0
0.02304	537.6	0.02158	664.4	0.01963	1043	0.02196	989.6
0.02314	536.9	0.02167	663.0	0.01972	1041	0.02206	988.3
0.02324	536.3	0.02176	661.7	0.01980	1040	0.02215	986.9
0.02333	535.6	0.02185	660.3	0.01988	1038	0.02224	985.5
0.02343	535.0	0.02195	659.0	0.01996	1036	0.02234	984.2
0.02353	534.3	0.02204	657.7	0.02005	1034	0.02243	982.8
0.02362	533.7	0.02213	656.4	0.02013	1033	0.02252	981.5
0.02372	533.0	0.02222	655.1	0.02021	1031	0.02261	980.2
0.02382	532.4	0.02231	653.8	0.02029	1030	0.02270	978.9
0.02391	531.8	0.02239	652.5	0.02037	1028	0.02279	977.6
0.02401	531.2	0.02248	651.2	0.02045	1026	0.02288	976.3
0.02410	530.6	0.02257	650.0	0.02053	1025	0.02297	975.1

(Contd.)

Table S6 (Contd.)

0.02419	530.0	0.02266	648.7	0.02061	1023	0.02306	973.8
0.02429	529.4	0.02275	647.5	0.02069	1022	0.02315	972.6
0.02438	528.8	0.02283	646.3	0.02077	1020	0.02324	971.3
0.02447	528.2	0.02292	645.1	0.02085	1018	0.02333	970.1
0.02457	527.6	0.02301	643.9	0.02093	1017	0.02342	968.9
0.02466	527.0	0.02309	642.7	0.02101	1015	0.02351	967.6
0.02475	526.4	0.02318	641.5	0.02109	1014	0.02359	966.4
0.02484	525.9	0.02327	640.3	0.02117	1012	0.02368	965.2
0.02493	525.3	0.02335	639.1	0.02124	1011	0.02377	964.1
0.02502	524.7	0.02344	638.0	0.02132	1009	0.02385	962.9
0.02511	524.2	0.02352	636.8	0.02140	1008	0.02394	961.7
0.02520	523.6	0.02361	635.7	0.02147	1006	0.02403	960.6
0.02529	523.0	0.02369	634.6	0.02155	1005	0.02411	959.4
0.02538	522.5	0.02377	633.4	0.02163	1004	0.02420	958.3
0.02547	522.0	0.02386	632.3	0.02170	1002	0.02428	957.1
0.02556	521.4	0.02394	631.2	0.02178	1001	0.02437	956.0
0.02565	520.9	0.02402	630.1	0.02186	999.4	0.02445	954.9
0.02574	520.3	0.02411	629.0	0.02193	998.0	0.02454	953.8
0.02583	519.8	0.02419	627.9	0.02201	996.6	0.02462	952.7
0.02591	519.3	0.02427	626.9	0.02208	995.2	0.02470	951.6
0.02600	518.8	0.02435	625.8	0.02215	993.9	0.02479	950.5
0.02609	518.2	0.02443	624.7	0.02223	992.5	0.02487	949.4

(Contd.)

Table S6 (Contd.)

0.02618	517.7	0.02452	623.7	0.02230	991.2	0.02495	948.4
0.02626	517.2	0.02460	622.7	0.02238	989.8	0.02504	947.3
0.02635	516.7	0.02468	621.6	0.02245	988.5	0.02512	946.2
0.02643	516.2	0.02476	620.6	0.02252	987.2	0.02520	945.2
0.02652	515.7	0.02484	619.6	0.02260	985.9	0.02528	944.1
0.02661	515.2	0.02492	618.5	0.02267	984.6	0.02536	943.1
0.02669	514.7	0.02500	617.5	0.02274	983.3	0.02544	942.1
0.02678	514.2	0.02508	616.5	0.02281	982.0	0.02552	941.0
0.02686	513.7	0.02516	615.5	0.02289	980.7	0.02561	940.0
0.02694	513.2	0.02524	614.6	0.02296	979.5	0.02569	939.0
0.02703	512.8	0.02531	613.6	0.02303	978.2	0.02577	938.0
0.02711	512.3	0.02539	612.6	0.02310	977.0	0.02585	937.0
0.02720	511.8	0.02547	611.6	0.02317	975.7	0.02593	936.0
0.02728	511.3	0.02555	610.7	0.02324	974.5	0.02601	935.1
0.02736	510.9	0.02563	609.7	0.02331	973.3	0.02608	934.1
0.02744	510.4	0.02570	608.8	0.02338	972.1	0.02616	933.1
0.02753	509.9	0.02578	607.8	0.02345	970.9	0.02624	932.1
0.02761	509.5	0.02586	606.9	0.02352	969.7	0.02632	931.2
0.02769	509.0	0.02594	605.9	0.02359	968.5	0.02640	930.2
0.02777	508.5	0.02601	605.0	0.02366	967.3	0.02648	929.3
0.02786	508.1	0.02609	604.1	0.02373	966.1	0.02655	928.3
0.02794	507.6	0.02616	603.2	0.02380	964.9	0.02663	927.4

(Contd.)

Table S6 (Contd.)

0.02802	507.2	0.02624	602.3	0.02387	963.8	0.02671	926.5
0.02810	506.7	0.02632	601.4	0.02394	962.6	0.02679	925.5
0.02818	506.3	0.02639	600.5	0.02401	961.5	0.02686	924.6
0.02826	505.9	0.02647	599.6	0.02408	960.3	0.02694	923.7
0.02834	505.4	0.02654	598.7	0.02415	959.2	0.02702	922.8
0.02842	505.0	0.02662	597.8	0.02421	958.1	0.02709	921.9
0.02850	504.5	0.02669	596.9	0.02428	956.9	0.02717	921.0
0.02858	504.1	0.02677	596.1	0.02435	955.8	0.02724	920.1
0.02866	503.7	0.02684	595.2	0.02442	954.7	0.02732	919.2
0.02874	503.3	0.02691	594.3	0.02449	953.6	0.02739	918.3
0.02882	502.8	0.02699	593.5	0.02455	952.5	0.02747	917.4
0.02889	502.4	0.02706	592.6	0.02462	951.4	0.02755	916.6
0.02897	502.0	0.02714	591.8	0.02469	950.3	0.02762	915.7
0.02905	501.6	0.02721	590.9	0.02475	949.3	0.02769	914.8
0.02913	501.2	0.02728	590.1	0.02482	948.2	0.02777	914.0
0.02921	500.8	0.02735	589.3	0.02489	947.1	0.02784	913.1
0.02928	500.3	0.02743	588.5	0.02495	946.1	0.02792	912.3
0.02936	499.9	0.02750	587.6	0.02502	945.0	0.02799	911.4
0.02944	499.5	0.02757	586.8	0.02508	944.0	0.02806	910.6
0.02952	499.1	0.02764	586.0	0.02515	942.9	0.02814	909.8
0.02959	498.7	0.02772	585.2	0.02521	941.9	0.02821	908.9
0.02967	498.3	0.02779	584.4	0.02528	940.8	0.02828	908.1

(Contd.)

Table S6 (Contd.)

0.02975	497.9	0.02786	583.6	0.02534	939.8	0.02836	907.3
0.02982	497.5	0.02793	582.8	0.02541	938.8	0.02843	906.5
0.02990	497.1	0.02800	582.0	0.02547	937.8	0.02850	905.6
0.02997	496.8	0.02807	581.2	0.02554	936.8	0.02857	904.8
0.03005	496.4	0.02814	580.4	0.02560	935.8	0.02865	904.0

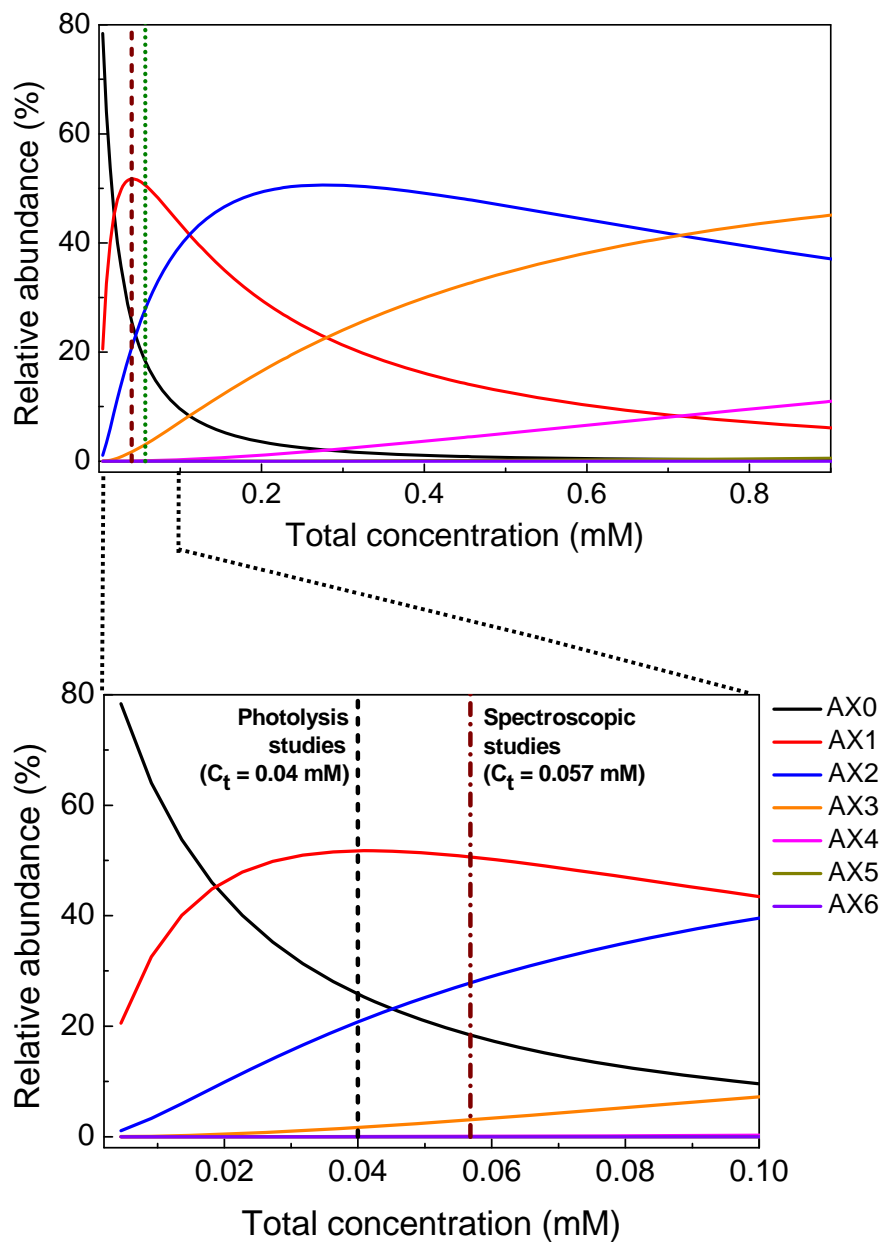


Fig. S7 The relative abundances of all the $\text{AX}_m^{(z-m)^+}$ species as a function of the total complex concentration (C_t) for $\text{RuMV2}(\text{PF}_6)_6 \cdot 2\text{H}_2\text{O}$ in aqueous media. The relative abundances under the conditions adopted in the spectroscopic and photolysis studies are listed in Table S7.

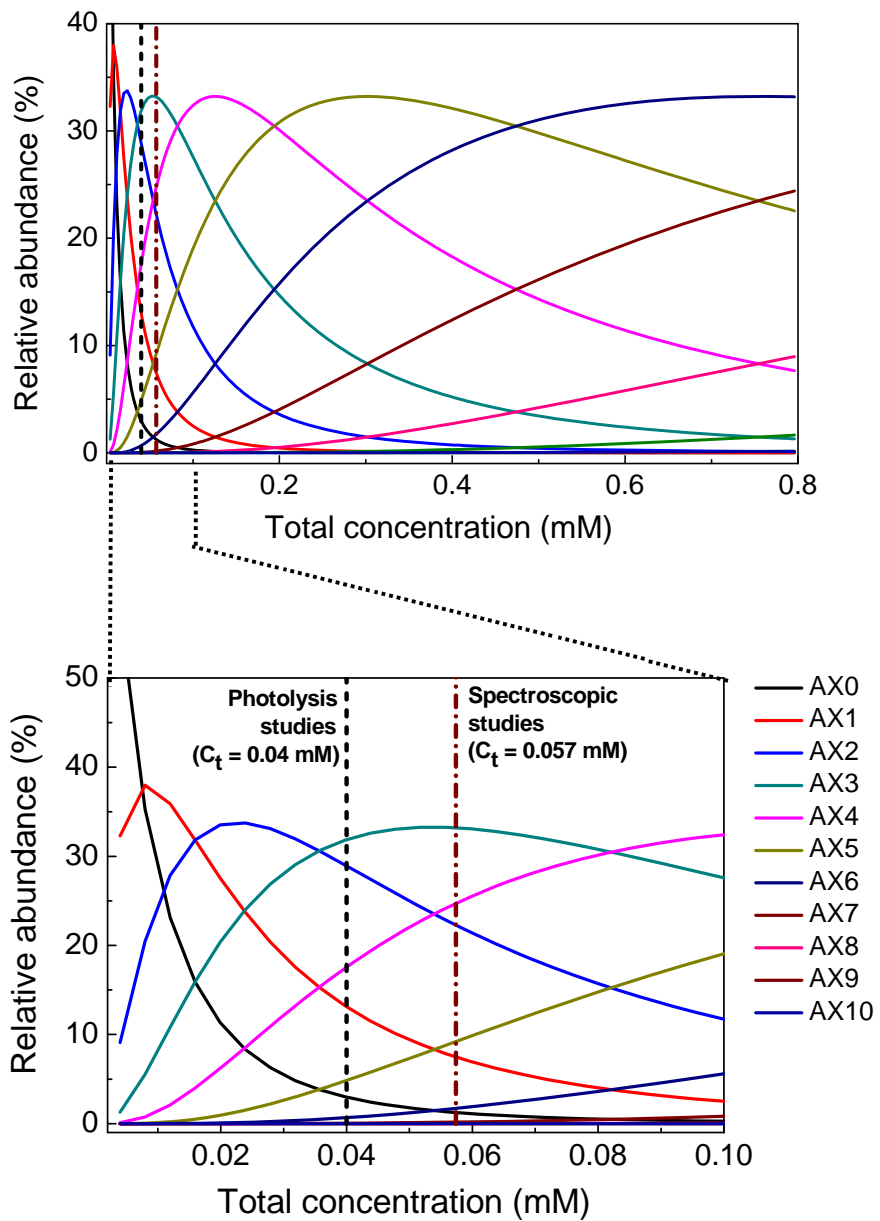


Fig. S8 The relative abundances of all the $\text{AX}_m^{(z-m)^+}$ species as a function of the total complex concentration (C_t) for $\text{RuMV4}(\text{PF}_6)_{10}\cdot\text{H}_2\text{O}$ in aqueous media. The relative abundances under the conditions adopted in the spectroscopic and photolysis studies are listed in Table S8.

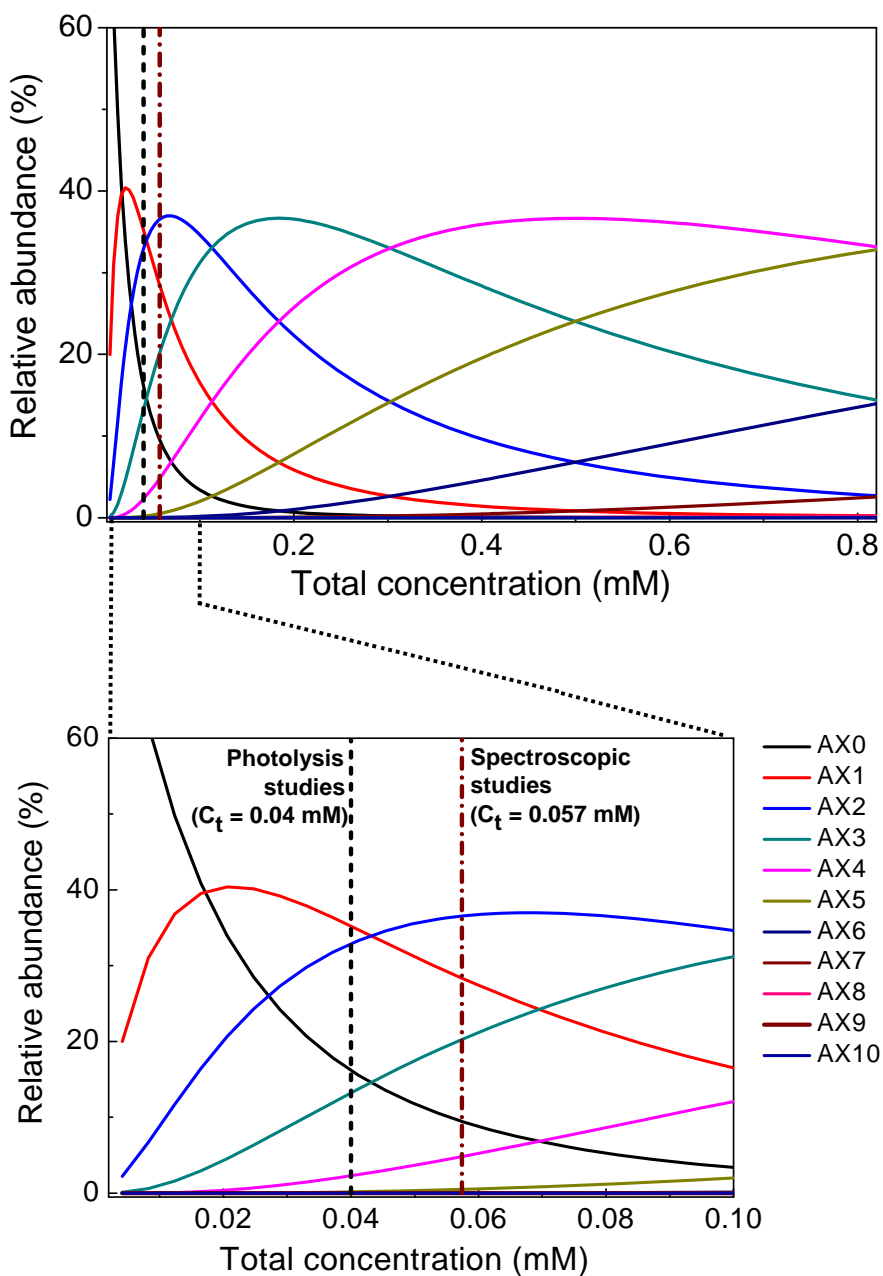


Fig. S9 The relative abundances of all the $\text{AX}_m^{(z-m)^+}$ species as a function of the total complex concentration (C_t) for $\text{RuMV4}(\text{Cl})_{10}$ in aqueous media. The relative abundances under the conditions adopted in the spectroscopic and photolysis studies are listed in Table S9, even though this compound was not employed in both studies.

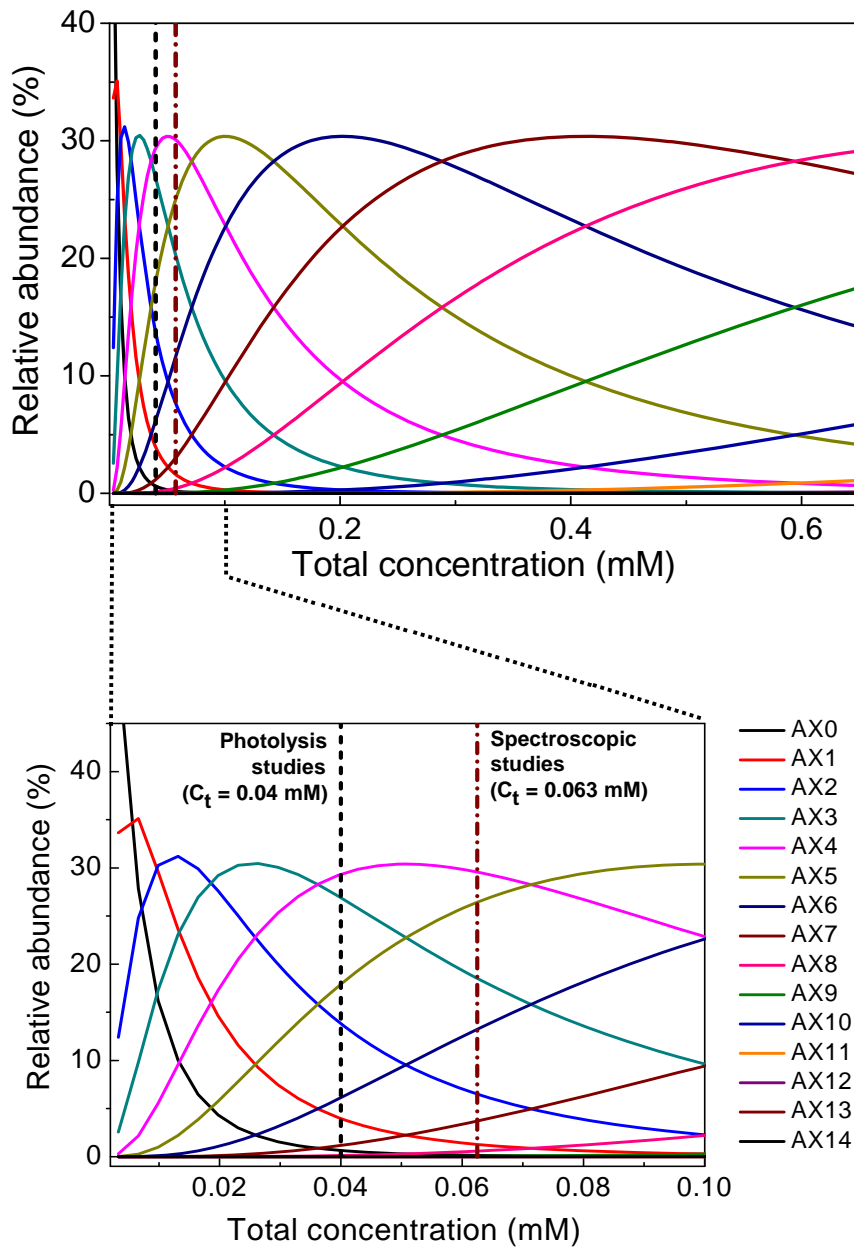


Fig. S10 The relative abundances of all the $\text{AX}_m^{(z-m)+}$ species as a function of the total complex concentration (C_t) for $\text{RuMV6}(\text{PF}_6)_{14} \cdot \text{H}_2\text{O}$ in aqueous media. The relative abundances under the conditions adopted in the spectroscopic and photolysis studies are listed in Table S10.

Table S7 The relative abundances of the chemical species for **RuMV2(PF₆)₆·2H₂O** in aqueous media under the conditions adopted in the spectroscopic and photolysis studies.

Chemical species	Spectroscopic studies (%) $C_t = 0.057 \text{ mM}$	Photolysis studies (%) $C_t = 0.040 \text{ mM}$
A^{6+}	17.7	25.3
AX^{5+}	50.3	51.8
AX_2^{4+}	28.6	21.2
AX_3^{3+}	3.26	1.73
AX_4^{2+}	7.42×10^{-2}	2.83×10^{-2}
AX_5^+	3.37×10^{-4}	9.26×10^{-5}
AX_6	3.07×10^{-7}	6.06×10^{-8}

Table S8 The relative abundances of the chemical species for **RuMV4**(PF₆)₁₀·H₂O in aqueous media under the conditions adopted in the spectroscopic and photolysis studies.

Chemical species	Spectroscopic studies (%)		Photolysis studies (%)	
	Ct = 0.057 mM	Ct = 0.040 mM	Ct = 0.057 mM	Ct = 0.040 mM
A ¹⁰⁺	1.35			3.01
AX ⁹⁺	7.87			13.2
AX ₂ ⁸⁺	22.9			29.0
AX ₃ ⁷⁺	33.2			31.8
AX ₄ ⁶⁺	24.2			17.5
AX ₅ ⁵⁺	8.78			4.79
AX ₆ ⁴⁺	1.60			0.657
AX ₇ ³⁺	0.145			0.451
AX ₈ ²⁺	6.58 × 10 ⁻³			1.54 × 10 ⁻³
AX ₉ ⁺	1.49 × 10 ⁻⁴			2.65 × 10 ⁻⁵
AX ₁₀	1.70 × 10 ⁻⁶			2.27 × 10 ⁻⁷

Table S9 The relative abundances of the chemical species for **RuMV4(Cl)₁₀** in aqueous media under the conditions adopted in the spectroscopic and photolysis studies.

Chemical species	Spectroscopic studies (%)	Photolysis studies (%)
	Ct = 0.057 mM	Ct = 0.040 mM
A ¹⁰⁺	9.38	15.5
AX ⁹⁺	28.3	34.7
AX ₂ ⁸⁺	36.6	33.3
AX ₃ ⁷⁺	20.4	13.8
AX ₄ ⁶⁺	4.88	2.45
AX ₅ ⁵⁺	0.503	0.187
AX ₆ ⁴⁺	2.23 × 10 ⁻²	6.14 × 10 ⁻³
AX ₇ ³⁺	4.24 × 10 ⁻⁴	8.66 × 10 ⁻⁵
AX ₈ ²⁺	3.47 × 10 ⁻⁶	5.26 × 10 ⁻⁷
AX ₉ ⁺	1.22 × 10 ⁻⁸	1.37 × 10 ⁻⁹
AX ₁₀	1.85 × 10 ⁻¹¹	1.54 × 10 ⁻¹²

Table S10 The relative abundances of the chemical species for **RuMV6(PF₆)₁₄·H₂O** in aqueous media under the conditions adopted in the spectroscopic and photolysis studies.

Chemical species	Spectroscopic studies (%)	Photolysis studies (%)
	Ct = 0.063 mM	Ct = 0.040 mM
A ¹⁴⁺	0.140	0.664
AX ¹³⁺	1.27	4.08
AX ₂ ¹²⁺	6.48	14.0
AX ₃ ¹¹⁺	18.5	27.1
AX ₄ ¹⁰⁺	29.6	29.2
AX ₅ ⁹⁺	26.4	17.7
AX ₆ ⁸⁺	13.3	5.98
AX ₇ ⁷⁺	3.72	1.13
AX ₈ ⁶⁺	0.584	0.120
AX ₉ ⁵⁺	5.14 × 10 ⁻²	7.15 × 10 ⁻³
AX ₁₀ ⁴⁺	2.53 × 10 ⁻³	2.38 × 10 ⁻⁴
AX ₁₁ ³⁺	6.99 × 10 ⁻⁵	4.44 × 10 ⁻⁶
AX ₁₂ ²⁺	1.05 × 10 ⁻⁶	4.63 × 10 ⁻⁸
AX ₁₃ ⁺	9.35 × 10 ⁻⁹	2.71 × 10 ⁻¹⁰
AX ₁₄	4.53 × 10 ⁻¹¹	8.86 × 10 ⁻¹³

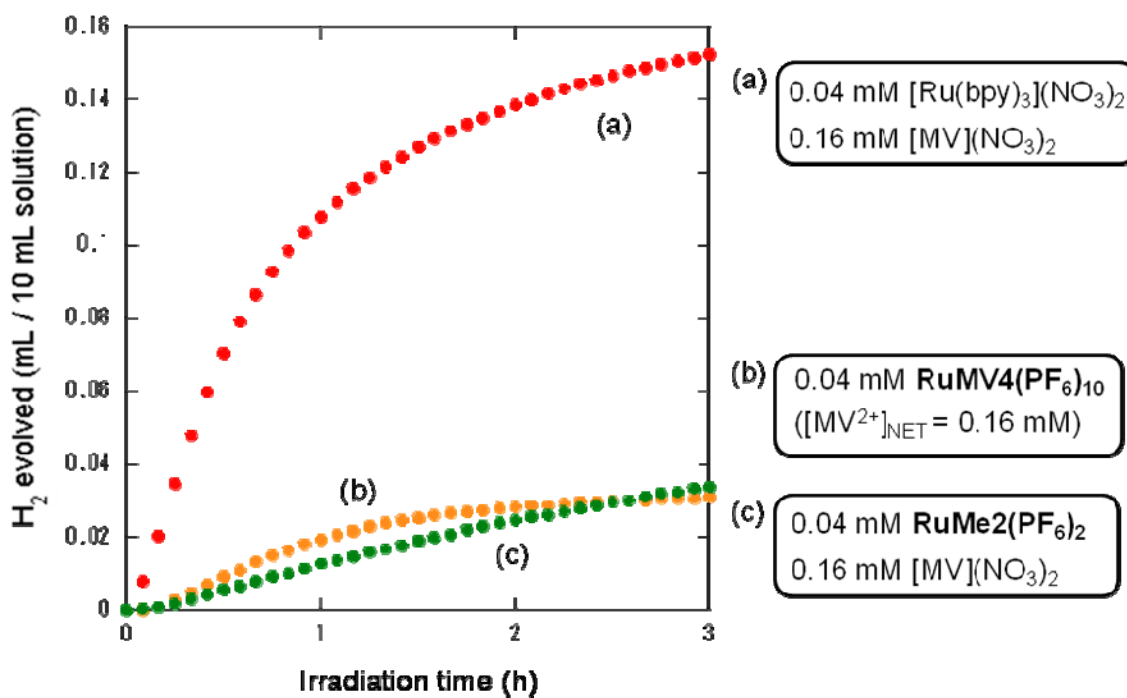


Fig. S11 Photochemical H₂ production from an aqueous acetate buffer solution (0.03 M CH₃COOH and 0.07 M CH₃COONa; pH 5.0, 10 mL) containing 30 mM EDTA and 0.1 mM *cis*-Pt(NH₃)₂Cl₂, under Ar atmosphere at 20 °C in the presence of additional components: (a) 0.04 mM [Ru(bpy)₃](NO₃)₂·3H₂O and 0.16 mM [MV](NO₃)₂; (b) 0.04 mM RuMV4(PF₆)₁₀ ([MV²⁺]_{NET} = 0.16 mM); (c) 0.04 mM RuMe2(PF₆)₂·H₂O and 0.16 mM [MV](NO₃)₂.

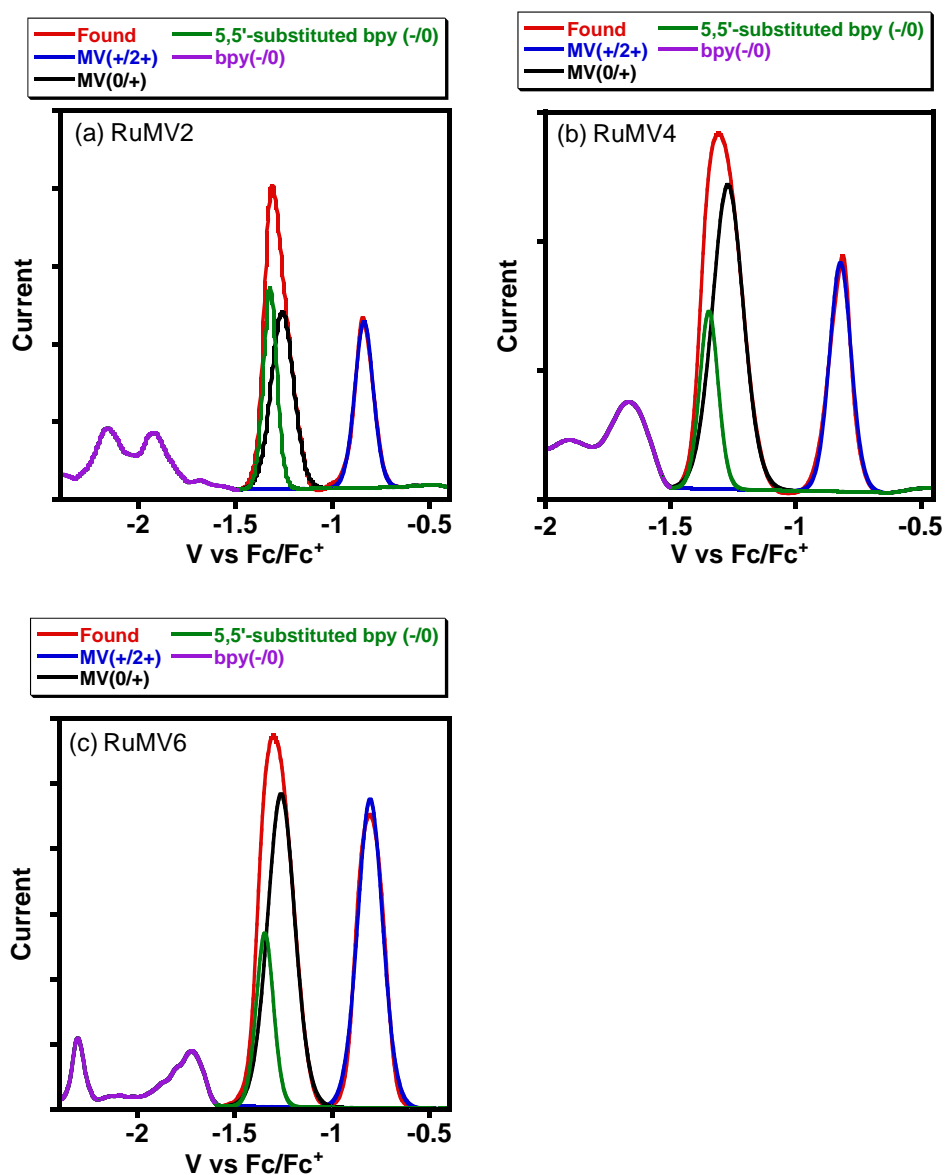


Fig. S12 Deconvolution studies on the differential pulse voltammograms of (a) **RuMV2**(PF₆)₆·2H₂O, (b) **RuMV4**(PF₆)₁₀·H₂O, and (c) **RuMV6**(PF₆)₁₄·H₂O. Experimental data are taken from those given in Fig. S4. For each case, deconvolutiton was carried out for the potential range where the successive one-electron reductions of viologen appear (-0.5 ~ -1.5 V vs. Fc/Fc⁺).

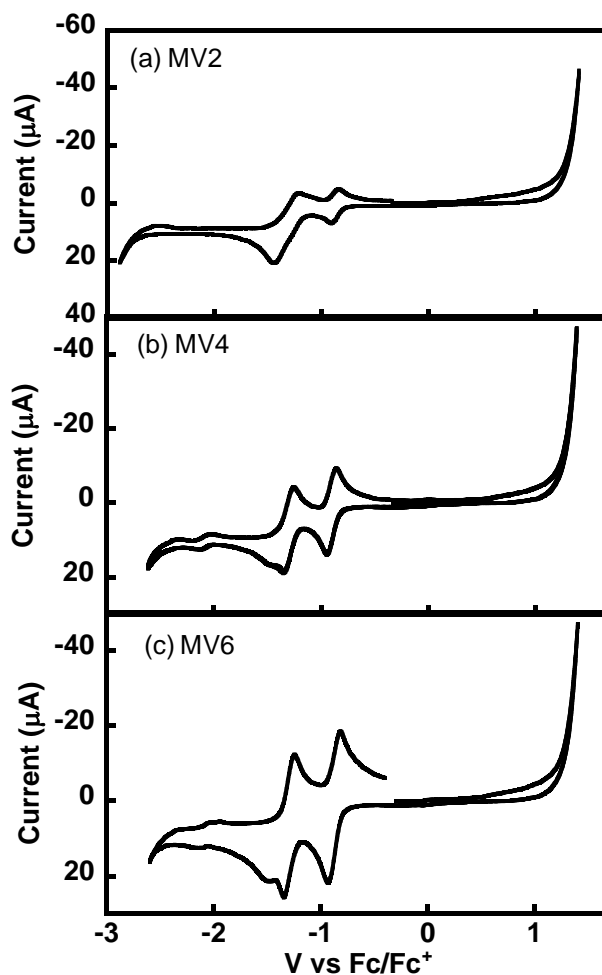


Fig. S13 Cyclic voltammograms of (a) **MV2**(PF₆)₄·2H₂O, (b) **MV4**(PF₆)₈·3H₂O, and (c) **MV6**(PF₆)₁₂·4H₂O (1 mM) in an acetonitrile solution containing 0.1 M TBAP (TBAP = tetra(n-butyl)ammonium perchlorate) at room temperature under Ar atmosphere. Each voltammogram was recorded at a sweep rate of 50 mVs⁻¹.

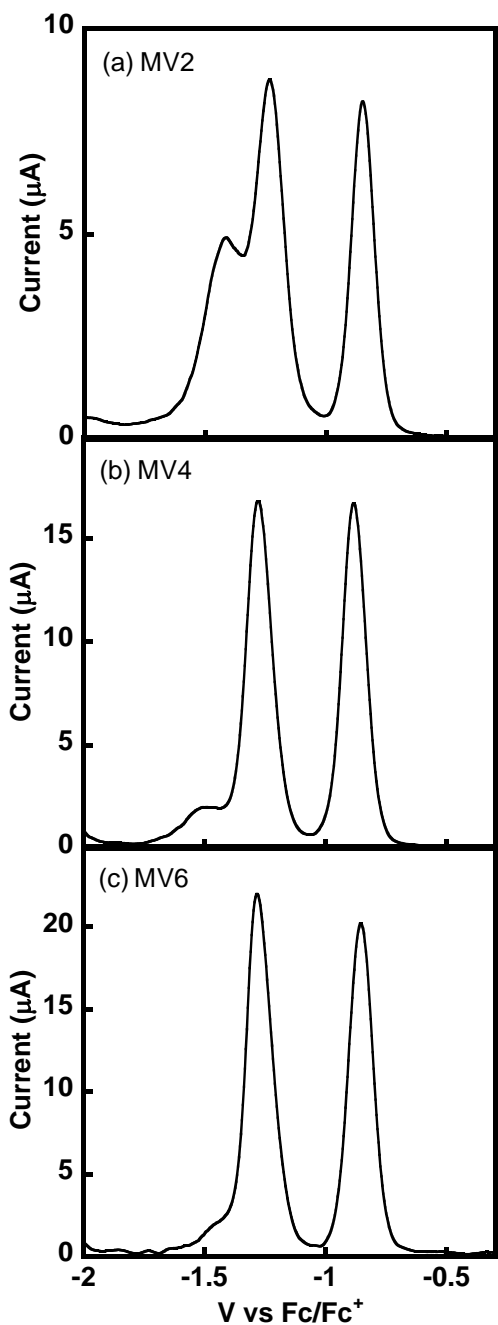


Fig. S14 Differential pulse voltammograms of (a) **MV2**(PF₆)₄·2H₂O, (b) **MV4**(PF₆)₈·3H₂O, and (c) **MV6**(PF₆)₁₂·4H₂O (1 mM) in an acetonitrile solution containing 0.1 M TBAP (TBAP = tetra(n-butyl)ammonium perchlorate) at room temperature under Ar atmosphere. Each voltammogram was recorded using a glassy carbon disk as the working electrode, at a sweep rate of 50 mVs⁻¹, a potential amplitude of 50 mV, and a step height of 4 mV.

References

- (1) S. E. Okan and D. C. Champeney, *J. Solution Chem.*, 1997, **26**, 405.
- (2) H. Yokoyama, K. Shinozaki, S. Hattori and F. Miyazaki, *Bull. Chem. Soc. Jpn.*, 1997, **70**, 2357.
- (3) E. Baumgartner, M. Busch and R. Fernández-Prini, *J. Phys. Chem.*, 1970, **74**, 182